Cobalt substituted lanthanide nickelates ($Ln_2Ni_{1-x}Co_xO_{4+\delta}$, Ln = La, Pr; x=0, 0.1, 0.2) as high performance oxygen electrodes for solid oxide cells

Vaibhav Vibhu, Izaak C. Vinke, Rüdiger- Albert Eichel, Jean-Marc. Bassat, L. G. J. de Haart

Cobalt substituted Lanthanide Nickelates ($Ln_2Ni_{1-x}Co_xO_{4+\delta}$, Ln = La, Pr; x = 0, 0.1, 0.2) as High Performance Oxygen Electrodes for Solid Oxide Cells

V. Vibhu[a], I. C. Vinke[a], R.-A. Eichel[a,b], J.-M. Bassat[c] and L. G. J. de Haart[a]

[a]Institute of Energy and Climate Research, Fundamental Electrochemistry (IEK-9), Forschungszentrum Jülich GmbH, 52425 Jülich, Germany
[b]Institute of Physical Chemistry, RWTH Aachen University, 52074 Aachen, Germany
[c]CNRS, Univ. Bordeaux, Bordeaux INP, ICMCB, UMR 5026, F-3360 Pessac Cedex, France

The present study is focused on the development of alternative oxygen electrodes for Solid Oxide Fuel Cells (SOFCs) and Solid Oxide Electrolyzers Cells (SOECs). Rare earth nickelates with general formula $Ln_2NiO_{4+\delta}$ (Ln = La, Pr or Nd) have shown good performance as oxygen electrodes with various electrolytes. To further enhance the physico-chemical properties, electrochemical performance as oxygen electrode and durability of Solid Oxide Cells (SOCs), herein, we have performed the substitution of nickel with cobalt in these nickelates. Two compositions (x=0.1 and 0.2) were mainly considered and completely characterized using several techniques. The single cells were then prepared and electrochemically characterized using DC- and AC-techniques in the temperature range 700-900 °C. The durability test up to 250h were also investigated at 1 $A.cm^{-2}$ current density at 800 °C under both SOFC (dry conditions) and SOEC conditions (with 50% H_2 and 50% H_2O feed gas mixture) indicating different degradation behavior.

Introduction

One of the biggest reasons for the climate change and global warming is the emission of CO_2 from fossil fuel which is increasing day by day in the earth's atmosphere. Consequently, it important to find eco-friendly technologies that use renewable fuel. A Solid Oxide Fuel Cells (SOFCs) are being considered as a novel power generation in future because of their very high energetic efficiency (by generating heat and electricity at the same time) without any pollution. On the other hand, Solid Oxide Electrolysis Cells (SOECs) have attracted considerable interest in the attainment of zero emission and high purity hydrogen production (1-3). Using high temperature SOECs, it is expected to consume less electrical energy as compared to electrolysis at low temperature as consequence of the more favorable thermodynamic and electrochemical kinetic conditions for the reaction. Commonly it is observed that, in Solid Oxide Cells (SOC) operation, electrode polarizations induce large voltage losses especially at the oxygen electrode, therefore the modification in the existing materials as well as investigation of new oxygen electrode materials are still under progress.

Mostly, two kinds of MIEC materials are used as oxygen electrodes; the first one concerns oxygen deficient perovskite materials *e.g.* LSCF ($La_{0.4}Sr_{0.6}Co_{0.8}Fe_{0.2}O_{3-\delta}$) or LSC ($La_{0.4}Sr_{0.6}CoO_{3-\delta}$). However, there are some disadvantages of these Sr-containing materials like Sr-segregation, high values of thermal expansion coefficients (TECs) (4) etc., lead to a degradation of the cell performances. Another type of MIEC oxides deals with oxygen over-stoichiometry, *e.g.* nickelates $Ln_2NiO_{4+\delta}$ (Ln = La, Pr, Nd). These compounds with the K_2NiF_4-type layered structure are promising due to their high anionic bulk diffusion as well as surface exchange coefficients, combined with good electrical conductivity and thermal expansion properties matching with those of yttria-stabilized zirconia (YSZ) or $Ce_{0.8}Gd_{0.2}O_{2-\delta}$ (GDC) used as electrolytes (5, 6). Moreover, $Pr_2NiO_{4+\delta}$ shows excellent electrochemical properties (7) but its chemical stability is always an issue (8-11), while $La_2NiO_{4+\delta}$ has a good chemical stability but with lower electrochemical performance (8).

So, in order to further enhance its overall electrochemical activity of oxygen electrode and durability of the SOCs, herein, we have prepared and characterized cobalt doped Lanthanum nickelates with general formula $Ln_2Ni_{1-x}Co_xO_{4+\delta}$ (Ln = La, Pr; x = 0.0, 0.1 and 0.2). In this study we have compared both the performance of these oxygen electrodes materials and the degradation behavior under operation in SOFC and SOEC conditions using single cells.

Experimental

Powder preparation, thermal ageing of powders and cell manufacturing

Three compositions of the $La_2Ni_{1-x}Co_xO_{4+\delta}$ (LNCO) and $Pr_2Ni_{1-x}Co_xO_{4+\delta}$ (PNCO) solid solution (x = 0.0, 0.1 and 0.2) were prepared using a solid state synthesis route. The corresponding precursors were La_2O_3 (Aldrich chem, 99.9%), Pr_6O_{11} (Sigma Aldrich, 99.9%), NiO (Alfa Aesar, 99%) and Co_3O_4 (Alfa Aesar, 99%). La_2O_3 and Pr_6O_{11} were pre-fired in a first step at T = 900 °C overnight to remove the water content, due to their high hygroscopic character, then to weight the exact amount of precursors. The precursors were weighed according to the composition of nickelates and then ball milled for 4h at 250 rpm using zirconia balls and isopropanol (VWR, 99.8%). After drying at 80 °C overnight, the final annealing was performed at 1300 °C for 12 h in air, leading to well crystallized phases. The obtained powders were crushed and milled again with zirconia balls and isopropanol for 8 h with the aim to obtain a mean particle size of about 1 μm (as checked using particle size distribution and SEM).

Powder Characterization

The powders were characterized by X-Ray diffraction (XRD) at room temperature using a PANanalytical X'pert MPD diffractometer with Cu-K_α incident radiation (λ = 1.5418 Å). Each X-ray diffractogram was fitted by profile matching using the Fullprof software. The morphologies of the materials were analyzed using a Scanning Electron Microscope (Quqnta FEG 650, FEI equipped with an EDS detector) operating at 10 kV. The particle size distributions for histograms were analyzed by laser diffraction particle size analyzer (HORBIA, LA-960).

Thermo-gravimetric analyses (TGA) were carried out using a TA Instrument® TA-Q5500 device in the temperature range 50 - 600°C, combining in a first step two cycles under air (with flow rate 2°C min^{-1}), then the last cycle under Ar - 4% H_2 (with a slow heating rate of 0.5°C min^{-1} up to 900°C). The first two cycles aim to check the thermal stability of the materials and to measure the oxygen over-stoichiometry changes under air upon heating, while the cycle under Ar - 4% H_2 lead to determine the oxygen stoichiometry at room temperature. Thermal variations of the relative expansion of the dense pellets (dL/L) were carried out in the temperature range 25 - 900°C with a heating and cooling rate of 2 °C.min^{-1} using a differential dilatometer (Netzsch® 402 ED), with the aim to determine the Thermal Expansion Coefficient (TEC) of the materials. The electrical conductivity of the materials was determined under air using the four-probe technique, in the temperature range 25−900 °C with the heating and cooling rate of 2 °C.min^{-1}. The nickelates were previously sintered at 1350 °C for 6 h in order to get dense pellets for the conductivity and dilatometry measurements.

Cell Preparation and Electrochemical Characterization

Commercial electrode supported half-cells (CeramTec®, ASC-10C type) made of a 300 µm thick NiO-8YSZ support (Ø = 20 mm), a 10 µm thick 8YSZ electrolyte membrane (Ø = 20 mm), a 3-4 µm thick GDC layer (Ø = 20 mm) were used to prepare the single cells. The oxygen electrode layers (Ø = 12 mm) *i.e.* nickelates were deposited by screen printing. The single cells comprised of LNCO electrodes were sintered at 1200 °C/1h and PNCO electrodes were sintered at 1150 °C/1h. These sintering temperatures were previously optimized to obtain a controlled homogenous porous electrode microstructure. After the preparation of oxygen electrode layer, a $LaNi_{0.6}Fe_{0.4}O_{3-\delta}$ (LNF) layer (Ø = 12 mm) was also deposited to improve the current collection (12).

For the measurement, gold and nickel grids (1.024 cm^{-2} mesh) were used as current collectors for oxygen electrode and fuel electrode respectively. The *i-V* curves and impedance diagrams were investigated from 700-900 °C temperature range. The *i-V* characteristics were measured in SOFC mode (OCV to 0.6 V, under dry conditions) and in SOEC mode (OCV to 1.5 V with 50 % H_2O and 50 % H_2 feed gas mixture). The impedance diagrams were recorded at OCV, 0.7 to 1.2 V in SOFC mode and from 1 to 1.5 V in SOEC mode with an increase of 0.1 V, under potentiostatic control with 50 mV *ac* amplitude, from 10^6 Hz down to 10^{-1} Hz, using IVIUM VERTEX potentiostat/galvanostat with integrated frequency response analyzer module. The complex impedance diagrams were fitted using an equivalent circuit by means of the RelaxIS® software. The polarization resistance R_p values were calculated from the difference between the low frequency (LF) and the high frequencies (HF) diagram intercepts with the real axis of the Nyquist representation.

Results and discussion

XRD Analyses

The XRD study shows that all these nickelates $La_2NiO_{4+\delta}$ (LNO), $La_2Ni_{0.9}Co_{0.1}O_{4+\delta}$ (LNCO10), $La_2Ni_{0.8}Co_{0.2}O_{4+\delta}$ (LNCO20), $Pr_2NiO_{4+\delta}$ (PNO),

$Pr_2Ni_{0.9}Co_{0.1}O_{4+\delta}$ (PNCO10) and $Pr_2Ni_{0.8}Co_{0.2}O_{4+\delta}$ (PNCO20) are single phases, their patterns being indexed with an orthorhombic cell. The cell of all LNCO (x = 0.0, 0.1 and 0.2) is described by the *Fmmm* and that of PNCO (x = 0.0, 0.1 and 0.2) is described by *Bmab* space group. Furthermore, full pattern profile matching was carried out using the FULLPROF software with the aim to find the lattice parameters. The lattice parameters of LNO and PNO are agreement with the previous reported results (13). The variation of lattice parameters and unit cell volume of LNCO and PNCO are plotted in Figure 1.

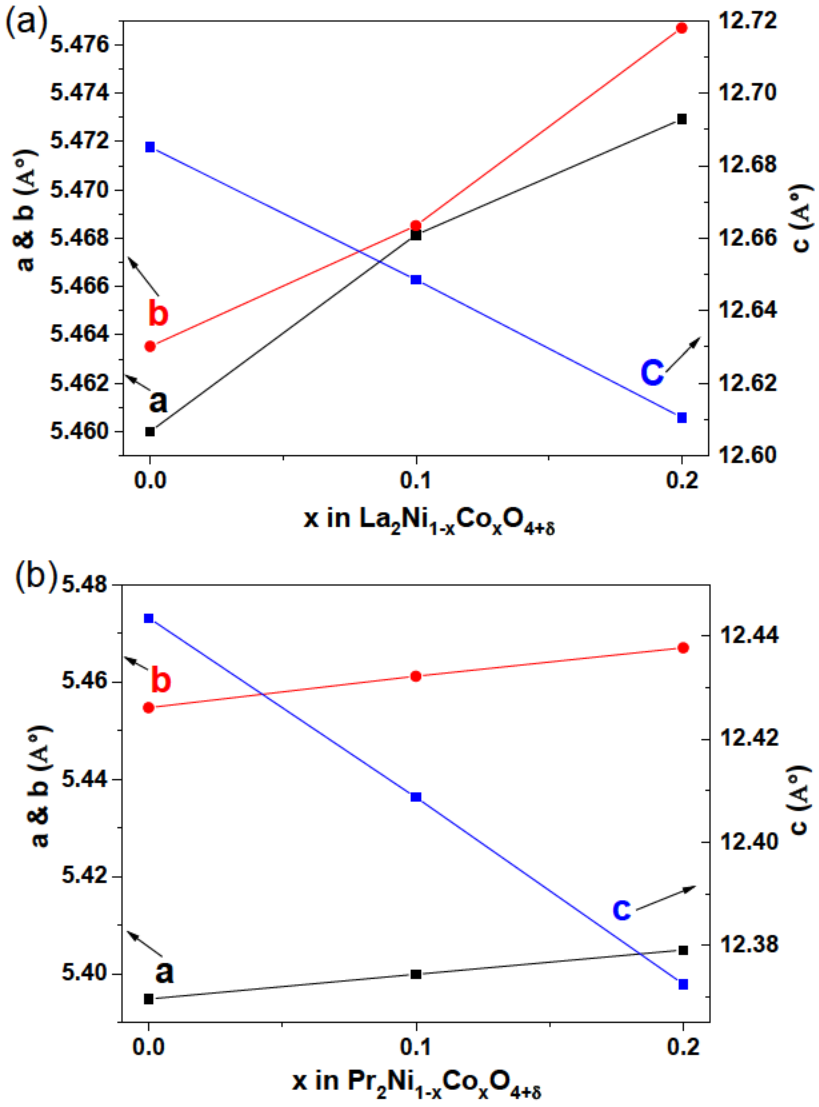

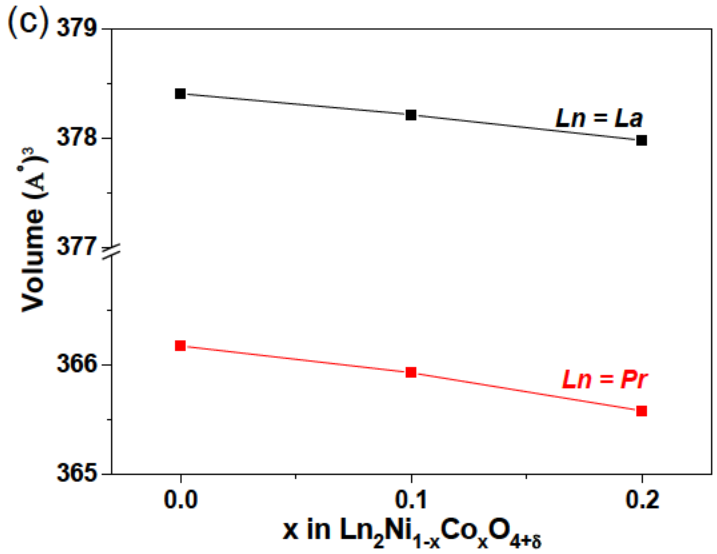

Figure 1. Variation of the lattice parameters as a function of *x*, for (a) $La_2Ni_{1-x}Co_xO_{4+\delta}$ (b) $Pr_2Ni_{1-x}Co_xO_{4+\delta}$ and (c) volume of unit cell.

In each case, an increase in the lattice parameters a and *b* is observed while a decrease is observed in lattice parameter c. The decrease in *c* is large compare to an increase in *a* and *b*, as a result the overall volume of the cell decreases with the cobalt substitution. This behavior is good agreement with the size of ionic radius of Co and Ni. As the ionic radius of Ni^{2+} (0.69 Å) is higher than Co^{2+} (0.65 Å), the cobalt substitution leads to decreases the overall volume of the cell.

Themogravimetry Analysis

The oxygen stoichiometry of the powders was thermodynamically equilibrated under air in the TGA device. For this purpose, the powders were heated up to 600°C and cooled down to room temperature with a slow heating rate (2°C min^{-1}) two times. The experiments show a reversible oxygen exchange, the second cooling is shown in Figure 2.

The oxygen over-stoichiometry (δ) of the all compositions were calculated using the results of a third TGA cycle performed under reducing conditions (4% H_2/Ar atmosphere). Two weight changes are observed: the first one occurs around 400°C, corresponding to the reduction of Ni^{3+}/Co^{3+} into Ni^{2+}/Co^{2+}. The second weight loss characterizes the complete reduction of the material, for instance the complete reduction of $La_2Ni_{0.8}Co_{0.2}O_{4+\delta}$ results in La_2O_3 and Ni and Co (confirmed by XRD). The δ values were calculated from both values of the weight changes. The results are listed in Table I, they have been used to graduate the Y-axis of Figure 2 (4+δ values). An increase of δ is evidenced with the increase of cobalt content for both La to Pr-nickelate.

TABLE I. Oxygen over-stoichiometry δ for $Ln_2Ni_{1-x}Co_xO_{4+\delta}$

Sample Name	δ (by TGA)
$La_2NiO_{4+\delta}$	0.16
$La_2Ni_{0.9}Co_{0.1}O_{4+\delta}$	0.18
$La_2Ni_{0.8}Co_{0.2}O_{4+\delta}$	0.20
$Pr_2NiO_{4+\delta}$	0.24
$Pr_2Ni_{0.9}Co_{0.1}O_{4+\delta}$	0.27
$Pr_2Ni_{0.8}Co_{0.2}O_{4+\delta}$	0.30

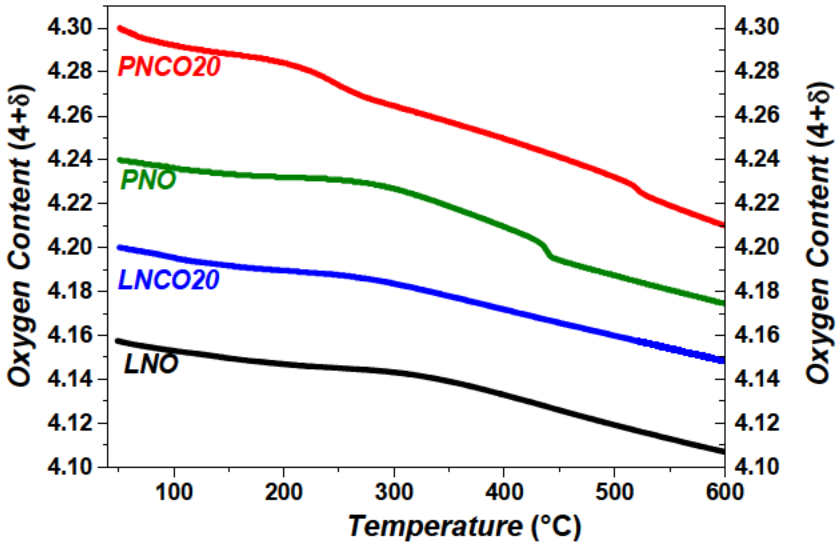

Figure 2. Thermal variation of the oxygen content (30°C ≤ T ≤ 600°C) for the $Ln_2Ni_{1-x}Co_xO_{4+\delta}$ (where Ln = La, Pr and x = 0.0 and 0.2), in air.

It is clear from the Figure 2 that all nickelates remain always oxygen over-stoichiometric within the entire temperature range up to 600 °C. A transition is observed at ~ 440°C for PNO and at ~ 520°C for PNCO20 because of a structural change from orthorhombic to tetragonal (14, 15), which is not evidenced for LNO and LNCO20.

Dilatometry Measurements

The thermal variations of the relative expansions dL/L measured for $Pr_{2-x}La_xNiO_{4+\delta}$, under air, are reported in Figure 3.

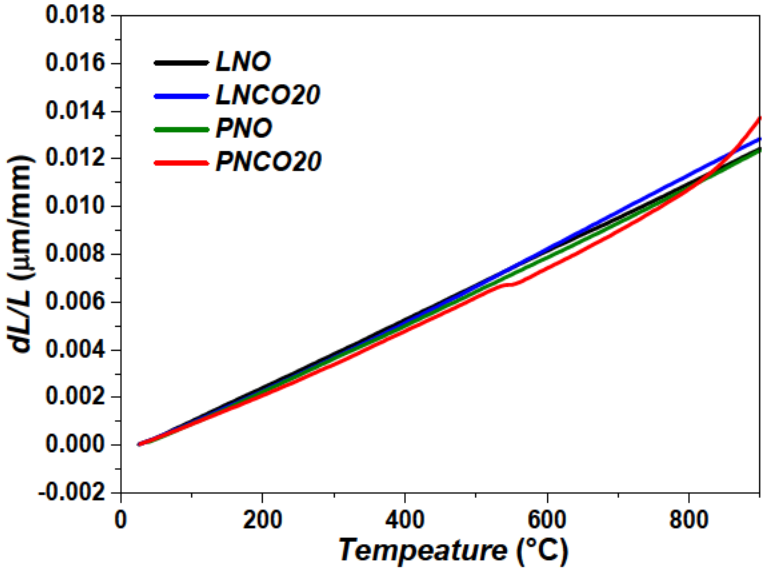

Figure 3. Thermal variation and relative expansion (dL/L) for $Ln_2Ni_{1-x}Co_xO_{4+\delta}$ (Ln = La, Pr and x = 0.0 and 0.2), under air ($30 \leq T \leq 900$°C).

They appear quite linear for LNO, LNCO20 and PNO and the thermal expansion coefficient (TEC) α have been calculated from the slope of the cooling curve. For example, the value of α are 13.2×10^{-6} °C^{-1}, 15.5×10^{-6} °C^{-1} and 13.5×10^{-6} °C^{-1} for LNO, LPNCO20 and PNO, respectively. The values for PNO and LNO are in good agreement with previous measurements (14, 16) and only slightly higher than that the one of 8YSZ (~11×10^{-6} °C^{-1}), indicating that from a thermo-mechanical point of view these nickelates can be used in SOCs devices with 8YSZ as electrolyte. For PNCO20, the curve is not linear especially above 800 °C and shows two kinds of slopes. However at temperature below 800 °C, the value of α ~ 13×10^{-6} °C^{-1} is observed for PNCO 20. Furthermore, for PNCO20, the same kind of transition as observed in TGA is also seen at ~ 440°C. Despite of the non-linearity of the relative expansion curve of PNCO20, no delamination of the oxygen electrode is noticed during the cell preparation (*i.e.* during the sintering process).

Electrical Conductivity Measurements

The variation of the total electrical conductivity σ *vs.* $1000/T$ under air for $Ln_2Ni_{1-x}Co_xO_{4+\delta}$ (Ln = La, Pr and x = 0.0 and 0.2) compounds is reported in Figure 4. All these materials exhibit semi-conducting behavior at least below 600 °C and among all the highest conductivity is observed for PNO.

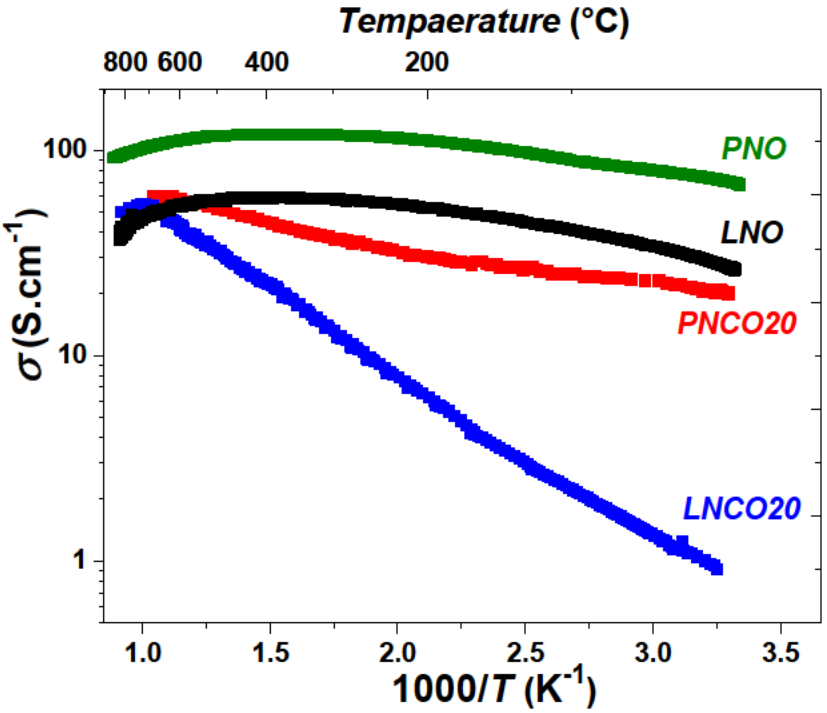

Figure 4. Thermal variation of the electrical conductivity measured under air for $Ln_2Ni_{1-x}Co_xO_{4+\delta}$ (Ln = La, Pr and x = 0.0 and 0.2).

With cobalt substitution a decrease in electrical conductivity is observed for both LNO and PNO. However for LNO and LNCO20 the value of electrical conductivity is similar at a temperature higher than 600 °C. On the other hand the conductivity value for PNCO20 is always lower than that of PNO. For instance, the conductivity of PNO and PNCO20 is 110 and 61 $S.cm^{-1}$ at 700 °C. Further raising the temperature leads to a decrease in the conductivity for all these materials, this pseudo-metallic behavior is directly correlated to the decrease of oxygen content as evidenced by TGA data and correspondingly to the decrease of the hole carrier density even though the compounds remain semi-conducting (17). Therefore it can be observed that in the case of nickelates, the substitution of Co at Ni-site does not improve the electrical conductivity contrary to the LSCF based perovskites materials (18).

Single Cell Characterization

The single cell was mounted into the measurement setup, with flows of air and N_2 on the oxygen and fuel electrode sides, respectively. The cell was heated at 900 °C and N_2 at the fuel side was progressively replaced by dry hydrogen (H_2) to reduce NiO into metallic Ni. The open circuit voltage (OCV) was around 1.2 V at dry conditions. The *i-V* curves and impedance diagrams of single cells were investigated from 700-900 °C temperature range. After the measurement under dry condition the electrochemical measurements were performed under humid condition at 800 °C with 50 % H_2O and 50 % H_2.

Figure 5 show the plots of *i-V* characteristics under SOFC and SOEC operation. An increase in performance is observed with Co-substitution in both SOFC and SOFC

mode and the best result is obtained with the single cell containing PNCO20 electrode. For instance, the maximum power density obtained for PNCO20 cell at 0.6 V is 1.2 W.cm^{-2} respectively at 800 °C, which is better than that of PNO, LNO, LNCO20 and the commercial LSCF cells.

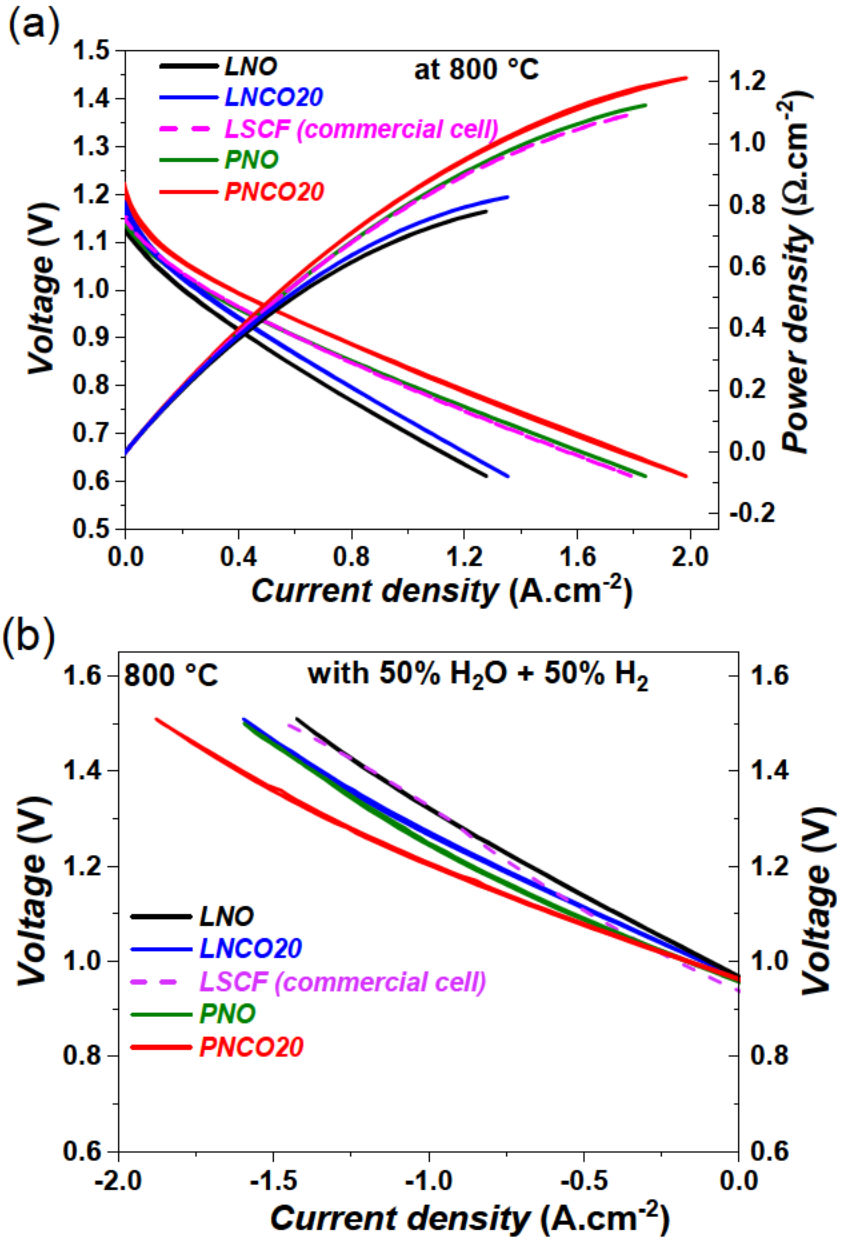

Figure 5. Current density-voltage relationship curves, at 800 °C for single cell containing $Ln_2Ni_{1-x}Co_xO_{4+\delta}$ (Ln = La, Pr and x = 0.0 and 0.2) and compared with commercial LSCF cell; (a) under SOFC mode and (b) under SOEC mode with 50% H_2 + 50% H_2O feed gas mixture.

In SOEC operation (Figure 5b) the commercial LSCF and LNO cell show almost similar performance. The LNCO20 cell has higher performance than LNO and similar to that of PNO cell. Remarkably, PNCO20 cell shows the best performance among all. For

instance, a maximum current density of 1.9 A.cm^{-2} is obtained at 1.5 V at 800 °C with 50% H_2 + 50% H_2O feed gas mixture.

The better performance of cobalt doped nickelates show better performance in both SOFC and SOEC modes even with the decrease in the electrical conductivity. It means that the electrochemical performance is not much dependent on the conductivity value. Then the difference in cell performance can be explained in terms of diffusion (D^*) and surface exchange coefficient (k^*) as these parameters are the key factors for the electrochemical performance of the materials. The values of both D^* and k^* is improved with the cobalt substitution. In the previously reported results it has been shown that even 10 or 20 % cobalt doping enhance the D^* and k^* values more than one order magnitude higher than the parent nickelate (5, 15, 19).

Long Term Stability Test under Fuel Cell and Electrolysis Conditions

The long term stability experiments were performed with the LNCO20 and PNCO20 electrodes containing single cells under SOFC conditions at 800 °C with high current density *i.e.* −1.0 A.cm^{-2} up to 250 h. The PNCO20 cell shows lower degradation comparison to the LNCO20 cell as depicted in Figure 6a. An estimated degradation rate (calculated from the slope of the linear part) of 98 and 238 mV.kh^{-1} is obtained for PNCO20 and LNCO20 cell respectively. The estimated degradation rate has quite high value (as first few hours are required for the stabilization) and could be expected lower when the cell will be operated longer.

The long term stability experiments were also performed under SOEC conditions (Figure 6b) at 800 °C with 50 % H_2O and 50 % H_2 at current density 1.0 A.cm^{-2} up to 250 h. Interestingly, a Co-doped nickelates containing single cell shows less degradation in comparison to LNO. The largest degradation is observed for LNO cell (113 mV/kh) and the most stable performance obtained with PNCO20 single cell with an estimated degradation rate of 22 mV/kh.

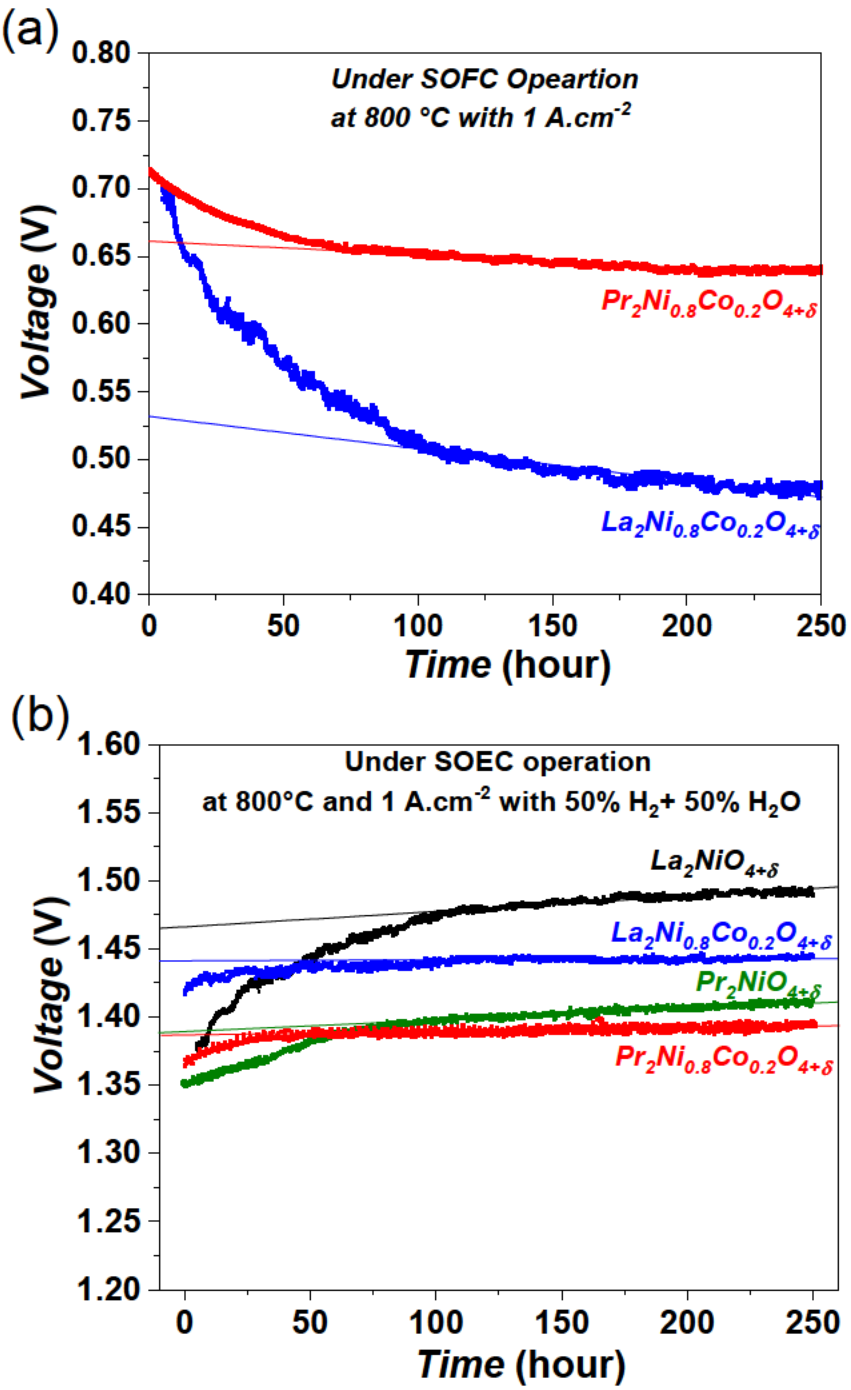

Figure 6. Long term stability test of single cells containing $Ln_2Ni_{1-x}Co_xO_{4+\delta}$ (Ln = La, Pr and x = 0.0 and 0.2) electrodes at 800 °C under current density of $\pm$1 A.cm^{-2}; (a) under SOFC operation and (b) under SOEC operation with 50% H_2 + 50% H_2O feed gas mixture.

Thus it is observed that degradation rate of these electrodes are lower in SOEC comparison to the SOFC operating conditions, indicates that these materials are even better for SOEC operation comparison to SOFC operation. The post-test analyses of these single cells are under progress in order to understand the degradation behavior.

Conclusions

This work was mainly dedicated to investigation of electrode materials $Ln_2Ni_{1-x}Co_xO_{4+\delta}$ (Ln = La, Pr and x = 0.0, 0.1 and 0.2) under both SOFC and SOEC conditions. These nickelates were successfully synthesized and characterized. From the structural point of view, all these nickelates crystallizes in orthorhombic structure. An increase in δ-value is observed with cobalt substitution for both LNO and PNO. The thermal expansion coefficients of all these nickelates are in between $13-15\times10^{-6}$ $°C^{-1}$. The electrical conductivity is decreases with cobalt substitution.

The single cell performance is improved with cobalt substitution in both SOFC and SOEC operating conditions. The best performance is observed for PNCO20 electrode containing single cell in both SOFC and SOFC mode. The long term stability test in SOFC operation shows high degradation rates than that of SOEC operation indicates that these nickelates based electrodes are even better candidates for SOEC than SOFC.

Acknowledgements

The results reported here were obtained within the frame of the European project SElySOs. This project has received funding from the Fuel Cells and Hydrogen 2 Joint Undertaking under grant agreement No 671481.

References

1. S. H. Jensen, P. H. Larsen and M. Mogensen, *Int. J. Hydrogen Energy*, **32**, 3253 (2007).
2. J. Udagawa, P. Aguiar and N. P. Brandon, *J. Power Sources*, **166**, 127 (2007).
3. A. Hauch, S. D. Ebbesen, S. H. Jensen and M. Mogensen, *J. Materials Chemistry*, **18**, 2331 (2008).
4. V. Vibhu, S. Yildiz, I. C. Vinke, R.-A. Eichel, J.-M. Bassat and L. G. J. de Haart, *J. Electrochem. Society*, **166**, F102 (2019).
5. C. N. Munnings, S. J. Skinner, G. Amow, P. S. Whitfield and I. J. Davidson, *Solid State Ionics*, **176**, 1895 (2005).
6. D. Pérez-Coll, A. Aguadero, M. J. Escudero, P. Núñez and L. Daza, *J. Power Sources*, **178**, 151 (2008).
7. C. Ferchaud, J.-C. Grenier, Y. Zhang-Steenwinkel, M. M. A. van Tuel, F. P. F. van Berkel and J.-M. Bassat, *J. Power Sources*, **196**, 1872 (2011).
8. V. Vibhu, J.-M. Bassat, A. Flura, C. Nicollet, J.-C. Grenier and A. Rougier, *ECS Trans.*, **68**, 825 (2015).
9. V. Vibhu, A. Flura, C. Nicollet, S. Fourcade, N. Penin, J.-M. Bassat, J.-C. Grenier, A. Rougier and M. Pouchard, *Solid State Sciences*, **81**, 26 (2018).
10. V. Vibhu, A. Rougier, C. Nicollet, A. Flura, S. Fourcade, N. Penin, J.-C. Grenier and J.-M. Bassat, *J. Power Sources*, **317**, 184 (2016).
11. A. V. Kovalevsky, V. V. Kharton, A. A. Yaremchenko, Y. V. Pivak, E. N. Naumovich and J. R. Frade, *J. Eu. Ceramic Society*, **27**, 4269 (2007).

12. M. C. Tucker, L. Cheng and L. C. DeJonghe, *J. Power Sources*, **196**, 8313 (2011).
13. V. Vibhu, M. R. Suchomel, N. Penin, F. Weill, J.-C. Grenier, J.-M. Bassat and A. Rougier, *Dalton Trans.*, **48**, 266 (2019).
14. A. Flura, S. Dru, C. Nicollet, V. Vibhu, S. Fourcade, E. Lebraud, A. Rougier, J.-M. Bassat and J.-C. Grenier, *J. Solid State Chem.*, **228**, 189 (2015).
15. C. Berger, E. Bucher, A. Egger, A. T. Strasser, N. Schrödl, C. Gspan, J. Hofer and W. Sitte, *Solid State Ionics*, **316**, 93 (2018).
16. V. Vibhu, A. Rougier, C. Nicollet, A. Flura, J.-C. Grenier and J.-M. Bassat, *Solid State Ionics*, **278**, 32 (2015).
17. J. M. Bassat, P. Odier and J. P. Loup, *J. Solid State Chem.*, **110**, 124 (1994).
18. E. V. Tsipis and V. V. Kharton, *J. Solid. State Electrochem.*, **12**, 1367 (2008).
19. J. A. Kilner and C. K. M. Shaw, *Solid State Ionics*, **154-155**, 523 (2002).